

Microfluidic Tissue Mesodissection in Molecular Cancer Diagnostics

SLAS Technology
 2017, Vol. 22(4) 425–430
 © 2016 Society for Laboratory
 Automation and Screening
 DOI: 10.1177/2211068216680208
journals.sagepub.com/home/jla



Christine Surette¹, David Shoudy², Alex Corwin¹,
 Wei Gao², Maria I. Zavodszky², Stanislav L. Karsten³, Todd Miller¹,
 Michael J. Gerdes², Nichole Wood², John R. Nelson², and Chris M. Puleo¹

Abstract

We present a mesodissection platform that retains the advantages of laser-based dissection instrumentation with the speed and ease of manual dissection. Tissue dissection in clinical laboratories is often performed by manually scraping a physician-selected region from standard glass slide mounts. In this manner, costs associated with dissection remain low, but spatial resolution is compromised. In contrast, laser microdissection methods maintain spatial resolution that matches the requirements for analysis of important tissue heterogeneity but remains costly and labor intensive. We demonstrate a microfluidic tool for rapid extraction of histological regions of interest from formalin-fixed paraffin-embedded tissue, which uses a simple and automated method that is compatible with most downstream enzymatic reactions, including protocols used for next-generation DNA sequencing.

Keywords

microfluidics, clinical automation, robotics and instrumentation, molecular biology, and genomics

Effective application of targeted therapeutics requires frequent profiling of a patient's tumor mutations.¹ However, plasma and tissue biopsies often have varying tumor content (ratio of tumor to healthy cells), which can confound standard genomic and proteomic assays.² Attempts to reduce tumor "contamination" by normal tissue are dominated by manual dissection methods, in which a technician physically scrapes away physician-defined regions of interest (ROIs) from glass slide tissue mounts. The delineation of these regions is typically performed by the physician after histological analysis of the tissue, which is stained for morphological examination with dyes such as hematoxylin and eosin (H&E). More advanced image processing, fluorescent imaging, and laser-based microdissection (i.e., dissection of 1–100 μm -sized ROIs) systems are all widely available, but the costs associated with these more refined techniques remain high. As an alternative, automated mesodissection (i.e., dissection of millimeter-sized ROIs) instruments are currently being developed to bridge the gaps between automation, ease of use, and cost.³

In parallel, with the drive for more cost-effective diagnostic instrumentation, there is also a great need to maximize the amount of data generated from trace or limited samples in costly drug discovery efforts and clinical trials. We have previously presented a multiplexed immunohistochemistry fluorescence-microscopy method for characterizing multiple analytes in individual formalin-fixed paraffin-embedded (FFPE) tissue samples.⁴ In this work, chemical inactivation of

fluorescent dyes after each image acquisition round allows reuse of common dyes in subsequent iterative staining and imaging cycles, greatly increasing the number of unique protein molecules that can be analyzed from the same tissue section. This technique has been integrated into a digital pathology platform, which includes accurate computation registration of the multiple sequential images. This allows digital segmentation of the tissue samples into cellular or subcellular compartments, providing information on the location and quantification of each of the multiplexed targets (demonstrated using up to 60 different proteins). In addition, this platform technology has been automated, and the reagent processing has been miniaturized to decrease the cost associated with multiplexed analysis.⁵

¹Electronics Organization, GE Global Research Center, Niskayuna, NY, USA

²Diagnostics and Biomedical Technologies, GE Global Research Center, Niskayuna, NY, USA

³NeuroInDx, Inc., Torrance, CA, USA

Unipick is a trademark of NeuroInDx.

Received Aug 18, 2016.

Supplementary material is available online with this article.

Corresponding Author:

Chris M. Puleo, PhD, Electronics Organization, GE Global Research Center, 1 Research Circle, Niskayuna, NY 12309, USA.

Email: puleo@ge.com

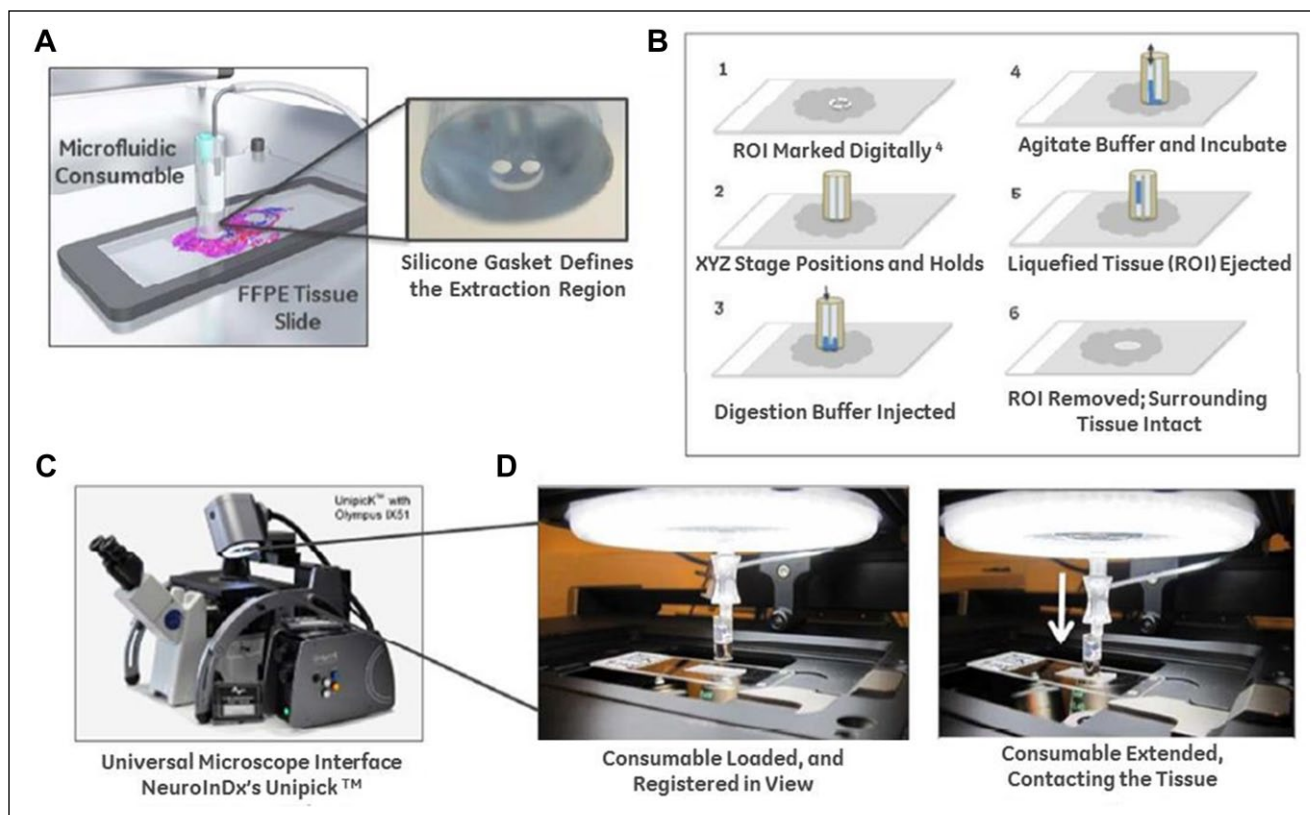


Figure 1. (A) The microfluidic consumable creates a gasket-enclosed microfluidic chamber on FFPE tissue samples. The silicone gasket defines the extraction region, and a magnetic or motor-driven force creates a hermetic seal around the ROI (further details on structure and manufacturing in SI ESI). (B) Schematic of the extraction protocol using the device and digestion buffer. (C) NeuroInDx's Unipick instrument, which can serve as a universal microscope interface for the microfluidic consumable. (D) Proof-of-concept integration of the microfluidic device with the Unipick, depicting the device loaded against a tissue slide during an extraction.

Herein, we extend the capabilities of the digital pathology platform to include a low-cost, easy-to-use microfluidic dissection tool for rapid extraction of ROIs for subsequent nucleic acid analysis. This gasket-enclosed extraction tool (GET) is capable of mesodissecting FFPE samples and incorporates advantages of laser-based dissection (i.e., automated tissue and cell selection and targeted extraction), while providing the economy and simplicity currently associated only with manual dissection.^{6,7} We also demonstrate that the GET can integrate into a universal cell and tissue acquisition system (Unipick, <http://www.neuroindx.com/products/unipick/>; NeuroInDx, Torrance, CA) that is easily operated on existing inverted microscopes. The combination of these two technologies form the basis of a dissection tool useful both in research labs seeking to gain a low-cost automated dissection tool and in clinical/commercial labs seeking to expand their dissection throughput capabilities.

Materials and Methods

Design of Microfluidic Tool

At the heart of the method is a microfluidic tissue extraction device consisting of a disposable tissue interface for delivering

and removing a “liquification cocktail” to a defined section of the tissue. This is attached to a metallic ring, which facilitates magnetically assisted contact of the bottom portion of the interface with the tissue (**Fig. 1A**). The details of the GET and the schematics of the overall extraction protocol are depicted in **Figure 1B**. The GET contains two microfluidic channels. The first channel (right) is connected through tubing to a pump that controls the transport of the tissue digestion/liquification reagent to and from the ROI. The second channel (left) is connected to a small reservoir designed to load the buffer and hold the final digested tissue suspension after ROI extraction. The bottom portion of the GET contains a variably sized silicone gasket (0.5–3 mm I.D.), which makes contact with the FFPE sample. The opening in this gasket connects the right and left microfluidic channels and completes the compartmentalized fluidic circuit (from outlet to reservoir) when pressed onto the tissue. The force applied to the gasket is controlled either by magnetic means (a pull force between a metal/magnet in the device and a corresponding paramagnetic/magnetic stage base) or by a displacement-controlled motor coupled to the device via a spring. The level of force is chosen to ensure negligible damage to the FFPE tissue beneath the gasket and a tight fluidic seal between the gasket and slide (additional

details on the device and force requirements for tissue extraction can be found in **Supplementary Material S1 ESI**. This simple microfluidic device can be integrated within the UnipicK platform for semiautomated x-y-z positioning using a standard inverted microscope (**Fig. 1C, D**).

Application and Testing of the Microfluidic Tool

To illustrate the capability of the GET, we used a 5 μm thick H&E-stained FFPE tissue section from a breast invasive ductal carcinoma biopsy and extracted 2-mm ROIs from targeted regions (**Fig. 2**). The slide has been manually annotated with 8 ROIs through microscopic examination by an internal pathologist (similar to a traditional manual dissection protocol in a clinical lab). A serial section was further processed and fluorescently stained using antibodies against Her2-cy5 and PR-cy3. Two sub-ROIs within the manually annotated region 1 (**Fig. 2A**) were then marked for mesodissection (**Fig. 2B**, top panel). The microfluidic device with the 2-mm gasket was positioned over each ROI and brought into contact with the tissue sample. A tissue digestion buffer was then automatically loaded into the microfluidic consumable from a reservoir (using the external pump) and selectively brought into contact with the tissue within the ROI gasket. Details on buffer composition can be found in **Supplementary Material S2 ESI**. Only the portion of the tissue within the opening of the gasket was exposed to the digestion buffer, and the size and shape of the gasket defined the portion of the tissue extracted. The tissue slide was heated to an elevated temperature optimal for the enzymatic activity within the buffer. The increased activity allows for shorter extraction time; however, room temperature is also effective. Once digested, the liquefied tissue sample (i.e., extracted ROI) was pumped back into the microfluidic consumable's reservoir, leaving a stripped region on the slide (**Fig. 2B**, bottom panel). The reservoir was placed into a microcentrifuge tube and centrifuged briefly to transfer the liquefied tissue sample from the device into the tube for downstream analysis. Repeated extractions were performed to evaluate the reproducibility of DNA yield across a separate colon tissue sample (image not shown; **Fig. 2C**). The extraction timing was also evaluated on a Xenograft SKV03 tissue sample (**Fig. 2D**).

The GET is a versatile device and can be integrated into preexisting commercial platforms, such as NeuroInDx's UnipicK microscope interface. In our example, the tool was attached to the UnipicK luer-lock consumable interface and anchored onto the platform to demonstrate proof-of-concept automation (**Fig. 1C, D**). In the UnipicK platform, the GET is aligned to an ROI using the system's x-y motion controls and then brought into contact with the tissue surface using the system's z-axis motion control (**Fig. 1D**). The z-axis motor can be used to control force applied to the gasket and create a fluidic seal on the slide, replacing the

paramagnetic stage base or magnet used in the independent microfluidic device (**Fig. 1A, B**). A transparent thin film heating insert or heated microscope slide stage can be used to directly heat the tissue sample and accelerate the tissue extraction.

Reagent and Immunohistochemistry Preparation

All FFPE tissue samples used in this report were purchased through Pantomics (Richmond, CA) and prepared for mesodissection through standard deparaffinization, rehydration, and antigen retrieval protocols. Prior to antibody staining, the tissue slides were blocked overnight in 10% donkey serum and stained with 4',6-diamidino-2-phenylindole (Thermo Fisher, Waltham, MA). After background imaging, the slides were stained with dye-conjugated monoclonal antibodies directed against human epidermal growth factor receptor 2 (Her2-cy5) and progesterone receptor (PR-cy3) and imaged again prior to extraction. The monoclonal antibodies used against Her2 (rabbit, anti-human) and PR (mouse, anti-human) were obtained from Cell Signaling Technology (Danvers, MA) and Dako (Carpenteria, CA) respectively, and conjugated with Cy3 or Cy5 at General Electric. The pre- and post-extraction fluorescent images demonstrate that the selective extraction of the ROIs using the microfluidic tool left no visible damage in surrounding tissue (**Fig. 2B**, bottom panel). The DNA extracted from the two ROIs was quantified, with background subtraction, using the Quant-iT HS assay (Thermo Fisher). Samples listed as xenografts were prepared after purchasing CD-1 nude mice or SCID mice from Charles River Laboratories (Wilmington, MA). Animals were housed under sterile conditions with food and water ad libitum and a 12 h light cycle. Mice were injected subcutaneously with 10^7 tumor cells in phosphate-buffered saline or culture medium while under 2% isoflurane anesthesia, and tumors were allowed to grow for approximately 5 to 10 d. Tumors were harvested, fixed, and prepared as described above for the purchased human samples. All animal studies were performed in accordance with federal and Institutional Animal Care and Use Committee guidelines using approved protocols.

Results and Discussion

DNA yield from the ROIs shown in **Figure 2B** (bottom panel) was 46.7 ng and 74.2 ng for ROI 1 and ROI 2, respectively. The difference in DNA yield between the two ROIs was consistent with the difference in cell density in those localized regions. A separate FFPE colon tissue slide with a more spatially uniform cell density was studied next to evaluate the reproducibility of the extractions' DNA yield. Four separate 2 mm ROIs across a single tissue slide were extracted, and their DNA content was quantified (**Fig. 2C**). The tight range of DNA yield across each of the four

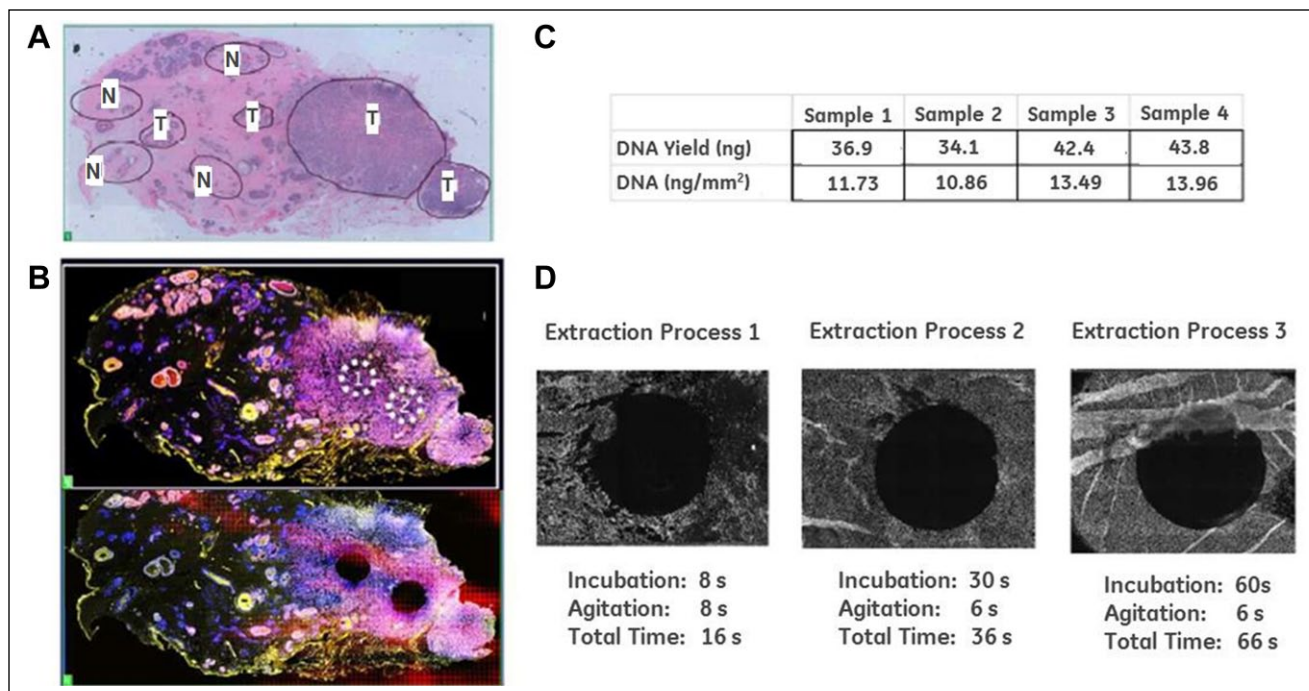


Figure 2. (A) Breast invasive ductal carcinoma formalin-fixed paraffin-embedded tissue sample stained with hematoxylin and eosin and tumor regions manually annotated by a trained pathologist (T = tumor region, N = area with normal or healthy tissue). (B) Pre-extraction and post-extraction images of a serial section tissue slide that was immunohistochemistry stained with HER2-CY5 and PR-CY3. The white circles indicate the regions annotated for extraction. Two 2 mm diameter regions were extracted from the annotated regions. (C) DNA yield from four 2 mm extraction regions across the same colon tissue slide. (D) Microscopic image of three different ROIs extracted using a range of digestion buffer incubation and agitation times.

samples (~34–44 ng) demonstrated extraction of reproducible concentrations of nucleic acids across the tissue.

The timing and completeness of the extraction were also evaluated. We found that at elevated temperatures, complete removal of the tissue within the gasket-defined ROI can be accomplished in seconds, making this method comparable to laser-based methods in terms of extraction speed (**Fig. 2D**; extraction process 1-3). Performing extractions at higher temperature may aid ROI removal in two ways. First, the activity of the enzymatic component of the tissue digestion buffer is optimal at higher temperatures (increased speed), and the higher temperatures may also aid in simple delamination of larger portions of tissue from the slide surface during the mechanical agitation associated with microfluidic loading of the ROI region with fluid. It should be noted that the speed of tissue digestion is dependent on the thickness of the tissue sample, as shown by the incomplete digestion of the thick tissue folds (an error in sample preparation) within the 60 s time point (**Fig. 2D**; extraction process 3). Additional details of the extraction protocol can be found in **Supplementary Material S2 ESI**.

Rapid tissue digestion and extraction are important in establishing a flexible dissection system that is capable of extracting irregular shapes and sizes of ROIs. Both laser-based and manual dissection methods allow for extracting

irregularly shaped regions preselected by physicians after histological analysis. Rapid tissue extraction within the GET enables serial dissection and generation of arbitrary shapes using sequential processing (overlapping ROIs). The GET can be moved from one location to the next, extracting a larger ROI with the same aliquot of digestion buffer or even multiple ROIs across the slide that exhibit a similar proteomic expression pattern of morphology. Alternatively, multiple GETs can be used to extract separate ROIs across a large tissue sample without cross-contamination. **Supplementary Figure S3** in **S1 ESI** demonstrates the capability of the GET to extract from multiple ROIs without loss of tissue due to damage surrounding the gasket feature.

Importantly, the microfluidic method of dissection and the digestion buffer remain compatible with downstream next-generation sequencing (NGS) workflows. After extraction and DNA quantification (as described above), 5 μ L of crude ROI extract was subjected to targeted resequencing. For comparison, DNA extracted from bulk tissue collected from whole FFPE slides of the same samples was also subject to targeted resequencing using the Ampliseq Cancer Panel (50 genes). Input DNA quantities used in the sequencing analysis were normalized to 10 ng from each sample, and DNA was determined amplifiable before

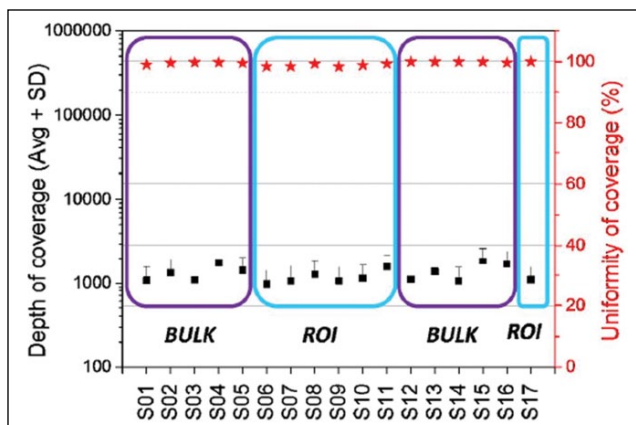


Figure 3. Samples from both data sets (whole slide [BULK] vs. dissected [ROI]) had very good depth of coverage. The descriptions of each samples listed along the x-axis (S01-S17) can be found in **Supplementary Material S3 ESI**, and they include both colon and breast cancer samples. Sequencing coverage describes the average number of reads that align to, or “cover,” known reference bases. The data show an average of 1000X to 2000X in both the amplified ROI and bulk samples (black data points). The uniformity of coverage (a measure of quantifying the evenness of the number of reads distributed across the entire region of interest) of the AmpliSeq samples was close to 100% (red data points). No significant effect was observed because of the multiplexing process⁴ (with or without bleaching, with or without antibody staining). Similarly, no significant differences were seen between the NGS results on the colon and breast cancer samples, indicating similar DNA quality (description of each sample S01–S17 found in **Supplementary Material S3 ESI**).

sequencing using a PCR-based assay for HBB gene primers (218 base-pair amplicon; post-DNA precipitation and preparation). Further details on integration into the sequencing workflow⁷ as well as a description of the sample and the data analysis protocol (including available or custom scripts for quality analysis, alignment, and statistical metric generation)^{8,10} are found in **Supplementary Material S3 ESI**. Excellent coverage and uniformity⁷ were accomplished using the DNA extracted from the ROIs, indistinguishable from the bulk samples (**Fig. 3**). No significant differences were seen across different types of tissues (i.e., colon or breast tissue samples) or after multiple rounds of antibody staining and protein imaging⁴ (staining data not shown). These results indicate that the microfluidic ROI extraction procedure (and reagents) provides DNA of adequate quantity and quality for NGS even from FFPE tissue samples that have been previously analyzed by immunohistochemistry. Current extensions of this work include the use of improved whole-genome amplification workflows to further decrease the amount of input DNA required, enabling extraction of submillimeter ROIs and use with other tissue samples including fine-needle aspirates.

With the growing use of advanced genomic and proteomic analyses of tumor samples for targeted cancer therapies, it is imperative that research and clinical laboratories have cost-effective methods of extracting the maximum amount of clinically useful information from the available trace or limited tumor samples.¹ FFPE tissue represents the largest pool of samples derived from clinical biopsies and pharmaceutical trials, yet researchers are challenged with either imprecise manual dissection techniques or costly and time-consuming laser-based microdissection for their analysis.^{11,12} In this report, we provide a simple-to-use and cost-effective approach of integrating automated dissection protocols into clinical workflows. Furthermore, we show proof-of-concept integration of our microfluidic FFPE dissection method with a commercially available cell extraction tool (UnipicK from NeuroInDx) that is back-compatible with a large range of inverted microscopes. Our demonstration shows that use of our device is compatible with advanced NGS workflows and provides flexibility for tissue dissection in terms of dissection speed and ROI shape and size. In future reports, we intend to expand the use of the microfluidic extraction technology within the fully digital molecular pathology platform previously developed^{4,5} and provide a complete platform to combine morphological, protein, and nucleic acid analysis using single FFPE samples.

Declaration of Conflicting Interests

The authors declared the following potential conflicts of interest with respect to the research, authorship, and/or publication of this article: S.L.K. is president and CEO of NeuroInDx. General Electric has filed a patent on the methods, consumable, and reagents described in this report.

Funding

Research reported in this publication was partially supported by the National Cancer Institute of the National Institutes of Health under Award Number R01CA194600 and R01CA174371 to MJG. The content is solely the responsibility of the authors and does not necessarily represent the official views of the National Institutes of Health.

References

1. Heuckmann, J. M.; Thomas, R. K. A New Generation of Cancer Genome Diagnostics for Routine Clinical Use: Overcoming the Roadblocks to Personalized Cancer Medicine. *Ann. Oncol.* **2015**, *26*, 1830–1837.
2. Smits, A. J. J.; Kummer, J. A.; de Bruin, P. C.; et al. The Estimation of Tumor Cell Percentage for Molecular Testing by Pathologists Is Not Accurate. *Mod. Pathol.* **2014**, *27*, 168–174.
3. Krizman, D.; Adey, N.; Parry, R. Application of Tissue Mesodissection to Molecular Cancer Diagnostics. *J. Clin. Pathol.* **2015**, *68*, 166–169.

4. Gerdes, M. J.; Sevinsky, C. J.; Sood, A.; et al. Highly Multiplexed Single-Cell Analysis of Formalin-Fixed, Paraffin-Embedded Cancer Tissue. *Proc. Natl. Acad. Sci. U.S.A.* **2013**, *110*, 11982–11987.
5. Clarke, G. M.; Zubovits, J. T.; Shaikh, K. A.; et al. A Novel, Automated Technology for Multiplexed Biomarker Imaging and Application to Breast Cancer. *Histopathology* **2014**, *64*, 242–255.
6. Fan, H.; Fulley, M. L. Chapter 2: DNA Extraction from Fresh or Frozen Tissues. In *Methods in Molecular Medicine*; Kileen, A. A., Ed. Totowa, NJ: Humana Press, 2001, p 49.
7. De Leng, W. J.; Gadella-van Hooijdonk, C. G.; Barendregt-Smouter, F. A. S.; et al. Targeted Next Generation Sequencing as a Reliable Diagnostic Assay for the Detection of Somatic Mutations in Tumors Using Minimal DNA Amounts from Formalin Fixed Paraffin Embedded Material. *PLOS One* **2016**, *11*(2), e0149405.
8. Andrews, S. FastQC: a quality-control tool for high-throughput sequence data. <http://www.bioinformatics.babraham.ac.uk/projects/fastqc/>.
9. Li, H.; Durbin, R. Fast and Accurate Long-Read Alignment with Burrows-Wheeler Transform. *Bioinformatics* **2010**, *26*, 589–595.
10. Li, H.; Handsaker, B. The Sequence Alignment/Map Format and SAMtools. *Bioinformatics* **2009**, *25*, 2078–2079.
11. Kokkat, T. J.; Patel, M. S.; McGarvey, D.; et al. Archived Formalin-Fixed Paraffin-Embedded (FFPE) Blocks: A Valuable Underexploited Resource for Extraction of DNA, RNA, and Protein. *Biopreserv. Biobank* **2013**, *11*, 101–106.
12. Muller, R.; Betsou, F.; Barnes, M.; et al. A Review from the International Society for Biological and Environmental Repositories (ISBER): Biospecimen Science Working Group. *Biopreserv. Biobank* **2016**, *14*, 89–98.